

Classification

Physics Abstracts

06.50 — 07.80 — 78.70

Curve fitting methods for quantitative analysis in electron energy loss spectroscopy

Tahar Manoubi, Marcel Tencé, Michael Gerard Walls (*) and Christian Colliex

Laboratoire de Physique des Solides, Bât. 510, 91405 Orsay Cedex, France

(Received December 15, 1989; accepted February 16, 1990)

Résumé. — Cet article présente une nouvelle approche pour déterminer les concentrations élémentaires dans les solides à partir de la spectroscopie des pertes d'énergie d'électrons (EELS). Cette méthode utilise des profils calculés des sections efficaces d'excitation des niveaux atomiques profonds et les représentations usuelles de variation du fond continu, afin de modéliser le spectre expérimental à la fois en dessous et au dessus du seuil caractéristique. Les pics intenses qui apparaissent dans certains cas juste au seuil ("lignes blanches") peuvent être simulés par des fonctions de Lorentz. Un algorithme d'ajustement aux moindres carrés détermine le poids des différentes composantes du modèle quand le meilleur accord avec le spectre expérimental est atteint. On peut prendre en considération la diffusion multiple en utilisant la partie basse énergie du spectre, dans une déconvolution du profil expérimental ou dans une convolution du profil simulé. Quand deux seuils sont analysés de cette façon, il est possible d'estimer ainsi les concentrations respectives des éléments concernés. Cette nouvelle approche est comparée pour quelques oxydes de fer et de chrome avec la technique habituelle de soustraction d'une loi extrapolée représentant le fond continu. Les deux méthodes fournissent des résultats satisfaisants pour les oxydes de fer si on tient compte des processus multiples. Cependant pour les oxydes de chrome, la proximité des deux seuils concernés (O-K et Cr-L) rend pratiquement impossible l'utilisation de la méthode de soustraction du fond continu alors que la modélisation décrite dans cet article donne des résultats proches des valeurs nominales. Cette approche originale devrait donc pouvoir être étendue avec succès à de nombreuses autres situations où un recouvrement notable des seuils considérés constitue une source de difficultés majeures pour l'analyse élémentaire quantitative en spectroscopie des pertes d'énergie.

Abstract. — A novel approach to the determination of elemental concentrations in solids by Electron Energy Loss Spectroscopy (EELS) is presented. The method uses calculated values of the inner-shell excitation cross-sections and standard assumptions about the form of the background, to model the spectrum before and after an excitation edge. Strong features just above the threshold (white lines) can be modelled by Lorentz oscillators. A least-squares fitting routine adjusts the weights of the various components of the model until the best fit with the experimental data is found. Multiple scattering can be taken into account by using the low-loss spectrum in a deconvolution with the experimental data, or in a convolution with the calculated spectrum. When two elemental edges are treated in this fashion, a value for their relative concentrations can be obtained. The method is compared with the conventional technique of background subtraction by pre-edge extrapolation, for the cases of some iron and chromium oxides. Both methods are found to give satisfactory results for the iron compounds if the effects of multiple scattering are included. However, for the oxides of chromium, the proximity of the two edges used (O-K and Cr-L) makes the use of the background subtraction method practically

(*) *Present address* : Cavendish Laboratory, Madingley Road, Cambridge CB1 0HE, G.B.

impossible, but the new approach gives results close to those expected from the chemical formulae. The method should prove applicable to a wide range of other problems in which overlapping edges are a problem.

1. Introduction.

Electron Energy-Loss Spectroscopy (EELS) is now an established technique in the analysis of the elemental composition of solids, especially in the context of electron microscopy and microanalysis [1, 2]. However, several problems remain in the process of extracting from the raw spectral data a figure for the absolute or relative concentration of a given atomic species. Firstly, the continuous falling background must be subtracted from the signal of interest for each element. Although this is known empirically to have the approximate form AE^{-r} in the majority of cases, the value of r may change from one part of the spectrum to another and is therefore difficult to determine precisely for the region under the excitation edge. Secondly, in order to relate the intensity in the spectrum to the number of atoms present, it is necessary to know the excitation cross-section (σ) for the atomic shell concerned either absolutely, or relative to those of the other elements present. The values of σ , which are function of the energy integration window Δ beyond the edge threshold, and of the acceptance angle β of the spectrometer, are either calculated using Hartree-Slater (H-S) methods [3] or hydrogenic models [4], or are measured from standard samples (see for example [5]). However, in the solid state, the variations in the density of states above the Fermi level can effectively change the value of $d\sigma/dE$ for a given atom and shell, especially in the first 50 eV above the threshold. Attempts have been made to take this into account in some of the calculations, but the full effect can never be included *a priori* for an arbitrary solid—especially if its composition is not exactly known. Thus, σ may be different in the material of interest from in a standard, or from the value calculated, and this will produce further errors in the result. Thirdly, the large cross-sections for outer shell excitations ($E = 0$ to 50 eV) mean that in samples of typical thickness (50 to 100 nm) there is an appreciable probability for multiple inelastic scattering, and the edges of interest are effectively convolved with the low-loss part of the spectrum, causing their shape to depart from that which would be obtained from an infinitely thin film. Finally, if two of the edges of interest are separated by less than about 100 eV the signals from the two elements concerned are partially superposed and there may be neither an adequate integration window Δ for the lower energy edge, nor a sufficiently large portion of spectrum of the form AE^{-r} before the edge at higher energy to enable a confident extrapolation to be performed.

The uncertainties introduced by these factors can limit the accuracy of the measurements to the order of 10 % or worse in some cases. Recently however, several workers have made attempts to overcome some of these difficulties. Steele *et al.* [6] have developed a method in which only the parts of the spectrum which are of known form (i.e. away from the edge thresholds) are used to determine the composition. Shuman et Somlyo [7] using standard edges and convolution techniques have detected concentrations of calcium of the order 10^{-4} % in biological samples (in which the edge shapes are practically constant) and Leapman and Swyt [8] have demonstrated how such a modelling approach can be effective in the quantification of overlapping edges, such as Ca-L_{2,3} on C-K, or S-L_{2,3} on P-L_{2,3}.

In this paper, we introduce the latest modifications and improvements to a technique which is in continuous development in our laboratory, namely that of modelling the entire pre-edge and edge region using a sum of functions each of which is supposed to represent a distinct contribution to the spectrum. We will first describe the new features of the method in detail, and then go on to

apply it to experimental test spectra from some oxides of iron and chromium. In all these cases the metal edge used displays strong “white line” resonances due to narrow dense bands of states, or bound states, just above the Fermi level. These materials thus represent a severe test of any quantification procedure applied.

2. The method.

The method consists of fitting the experimental data over a large energy range, encompassing both the pre-edge and post-edge domains, with a model curve comprising a sum of theoretical functions. An iterative least-squares fitting routine based on “Curfit” described by Bevington [9] is used. A simplified expression for the simulated intensity $F(E)$ at energy-loss E , to be compared with the experimental spectrum $I_{\text{exp}}(E)$, can be written as :

$$F(E) = AE^{-r} + \lambda_1\sigma_1(E) + \lambda_2\sigma_2(E) + \dots \quad (1)$$

The monotonically falling background is modelled by the conventional AE^{-r} function, the transitions for different core edges (1, 2,...) by a choice of cross-sections σ_1 and σ_2 described below. The concentration ratio of the two elements is governed by the weighting parameters λ_1 and λ_2 . More specifically, as described in earlier publications [10, 11], each edge can be described as the sum of different contributions ; for instance, in the case of L edges in transition metals, one can discriminate between the transitions to continuum states and the intense white lines modelled by Lorentzian (or Gaussian) terms. The floating parameters therefore include A and r for the background, the position weight and width of the Lorentzians, and the weight and positions of the continuum functions which may in fact themselves be a sum of two curves of the same shape (for example in an L edge the L_2 and L_3 contributions can be made independent). However, various constraints can be introduced, either from physical considerations, or to speed up to calculation, and these will be discussed for each case where they are applied.

Two major improvements have been made in the last few months. The first concerns the function used to describe transitions to the continuum. In [10] they were modelled by an arctangent of variable width and position. The choice was based on computational simplicity and had no physical significance. Nevertheless, it usually proved adequate, in conjunction with the Lorentz oscillators, when the aim of the experiment was to measure the white line strengths near the threshold. But for elemental quantification, the edges need to be fitted more accurately over a region of perhaps 100 eV, in which the decreasing tail cannot be reproduced by the step-like arctan function. This has therefore been replaced by theoretical atomic cross-sections calculated using H-S methods, which can be applied to any edge, including the $M_{4,5}$ excitation in the lanthanides [11]. Such a calculation can be performed for a given value of β and accelerating voltage E_0 in about one minute on the PDP11 computer used, and the more commonly needed results are stored in files, which means that the time required to perform the analysis is not greatly increased. Because the cross-sections have an absolute magnitude, their weight in the final fit gives a direct indication of the number of atoms in the beam path (if the intensity of the zero-loss peak is also known) or more usually, the ratio of the concentration of any two or more elements whose edges are modelled in this way. A further advantage accruing from this general approach is that if two of the thresholds are too close together to permit a background extrapolation for the one at high energy loss, both may be quantified simultaneously, using all the relevant contributions to the two edges, but just a single background function.

The second improvement is the incorporation into the algorithm of the option of convolving the fit with the low energy-loss part of the spectrum (usually from 0 to about 100 eV). Such a convolution, when performed on the model before comparison with the real spectrum, at each

iteration, simulates the effect of multiple inelastic scattering, which, as mentioned earlier, is a common source of error. The basic equation then becomes ;

$$F(E) = \{AE^{-r} + \lambda_1\sigma_1(E) + \lambda_2\sigma_2(E) + \dots\} * I_1(E) \quad (2)$$

where $I_1(E)$ is the low-loss spectrum.

Figure 1, showing a typical spectrum from a FeO specimen, illustrates how the technique, derived from equation (2), is applied. The low loss term $I_1(E)$ is displayed in figure 1a from 0 to 150 eV with its absolute intensity scale and the zero loss peak non saturated. The detailed behaviour of the inelastic component with its plasmon at 25 eV and the Fe M_{23} edge at 55 eV is shown in an insert. This experimental function is used for convolution. The model spectrum corresponding to the term within { } in equation (2) is displayed in figure 1b. It consists of the superposition of four contributions : a) a regularly decreasing background $A \cdot E^{-r}$, the parameters involved A and r corresponding to the best fit over the whole range of energy losses investigated and not only over a pre-edge domain ; b) a H.S. model cross section for the oxygen K edge ; c) a H.S. model cross section for the iron L_{23} edge ; d) a pair of Lorentzian peaks to model the white lines.

At this point, it must be emphasized that the H.S. calculations only deal with transitions to unoccupied continuum states and do not take into account transitions towards bound states involved in the white lines. This is why we feel necessary to consider explicitly the white lines in the fitting process, in contrast with the Steele *et al.* [6] approach which avoids certain regions of the data close to threshold, where the fit is poor. One important aspect of the present work is to use all available data and not only part of them. The need to introduce Lorentzians (or other line shape functions) to reproduce the narrow and intense features close to the edge, may be questioned because the atomic ratio is actually determined by the ratio of the H.S. cross sections. Two arguments can be evoked to justify extending the fit into the white lines spectral domain. Firstly, for medium to thick specimens such as are analysed in this paper, the detailed shape of the continuum on the iron L_{23} edge, results from the superposition of the H.S. cross section and of the convolution of the white lines with the low energy loss function. Secondly, it is important to estimate the weight of the white lines, individually or together, and to compare it with that of the continuum transitions, for instance to evaluate the number of vacancies in the d-band, see Pearson *et al.* [12]. The final stage of the fitting process is shown in figure 1c, after convolution of the model spectrum (made of the best combination of individual components) with the low loss spectrum of figure 1a. Apart from fine oscillating structures on the oxygen K edge which are not dealt with in the present description, there exists a very satisfactory agreement between the experimental and the model spectra, which can be checked through the value of the χ^2 factor.

. Other benefits and disadvantages of this approach involving a convolution to handle thicker specimens, as opposed to conventional methods using deconvolution of experimental data, will be discussed later.

The convolution is carried out in 'real space' —i.e. Fourier techniques are avoided—. This makes the process a little slow, but removes the need for rounding off the ends of the low-loss data, and avoids the problem of how to make a continuous, periodic function from the simulated spectrum, which would arise if for example Fourier-ratio techniques were used. As with all convolutions and deconvolutions of this kind, the low-loss spectrum must have an unsaturated zero-loss peak, and must be acquired under the same experimental conditions (accelerating voltage, angles of convergence and collection) as the edge spectra. Also, all the experimental data must be acquired from regions of the same thickness (preferably all from the same area), and with no contamination or beam-damage occurring.

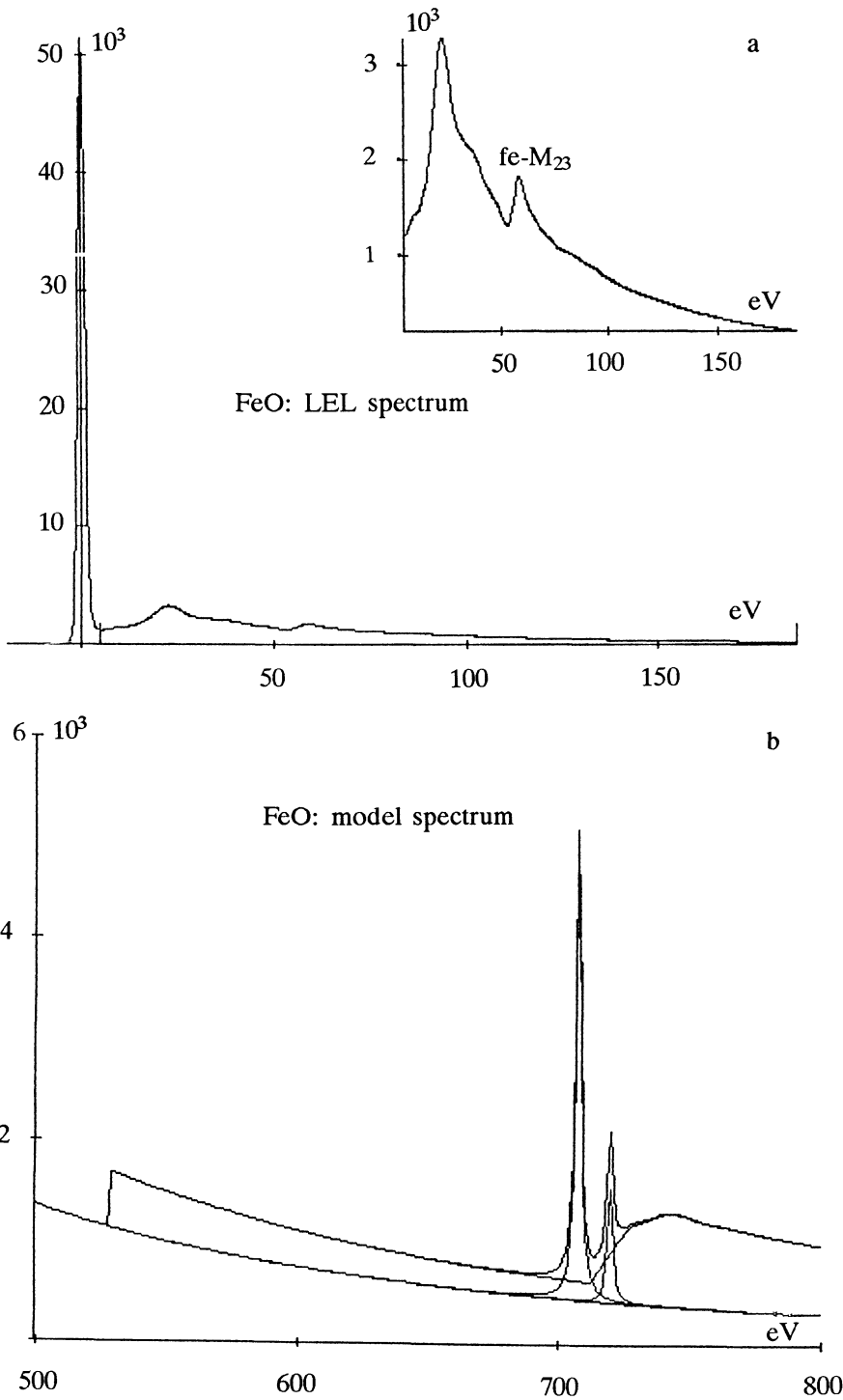


Fig. 1. — The low-loss spectrum of FeO (a) can be convolved with a calculated version of the single scattering distribution in the region of the O-K and Fe-L edges (b) to produce a curve which closely resembles the experimental spectrum in that region (c).

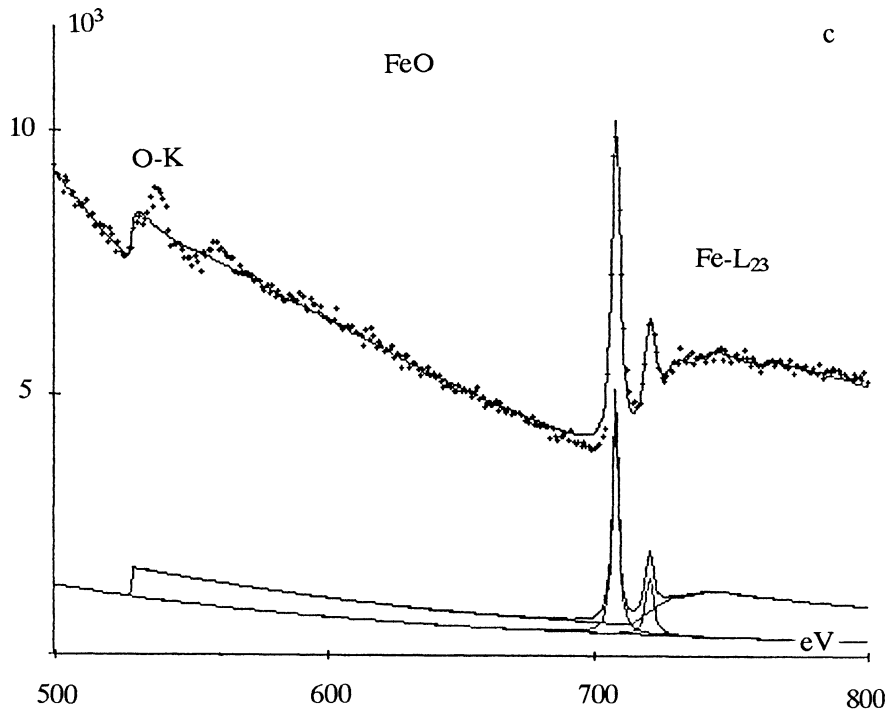


Fig. 1. — (continued).

The process described in equation (2) consists of replacing the contents $F(E)$ of each channel E in the fit with the quantity

$$\sum_{E_1} F(E - E_1) I_1(E_1) \quad (3)$$

where the E_1 are the low-loss channel energies, extending to E_f which is of the order of 100 eV, and the I_1 are their contents after the normalization

$$\sum_{E_1} I_1(E_1) = 1 \quad (4)$$

This clearly requires the existence of E_f channels in the unconvolved fit before the part corresponding to the real spectrum. These are filled by a reverse extrapolation of the AE^{-r} curve which can lead to very large numbers in the channels at lowest energy. This could cause problems when dealing with edges at rather low energy-loss for which such an extrapolation may extend into the low-loss part of the spectrum, or even below, where the AE^{-r} function is obviously no longer valid. In such cases a Fourier-log process would probably be the most suitable. Here however, we will treat no edges below the oxygen-K at 532 eV. The process as described is also only valid when the channel spacings ΔE are the same in the two parts. If necessary the low-loss spectrum can be converted to meet this condition.

3. Application of the method to transition metal oxides.

We will now apply the conventional and the new methods to the spectra of some iron and chromium oxides. In both groups there are considerable solid-state modifications to the edge shapes of both the oxygen (K) and transition metal (L). In the case of chromium there is also a severe overlap problem, the L_3 peak arising at around 577 eV (just 45 eV after the O-K). These materials thus illustrate some of the major difficulties in the process of quantification.

3.1 EXPERIMENTAL. — The iron oxides examined were $Fe_{1-x}O$ ($x \ll 1$), alpha and gamma type Fe_2O_3 and Fe_3O_4 . All were prepared in the form of thin films by vacuum evaporation followed by the appropriate thermal treatment [13]. Chromium dioxide particles were removed from the surface of a BASF audio-cassette tape onto a holey carbon film for direct microscope observation. Laboratory standard Cr_2O_3 powder was also examined on a holey carbon film after crushing.

The EELS experiments were performed in a VG HB5 Scanning Transmission Electron Microscope (STEM) fitted with a Gatan 607 Electron Spectrometer. The STEM uses a convergent incident beam (semi-angle in this work 15 mrad) and the value of collection angle β was 25 mrad, yielding an effective collection angle β^* of 22.6 mrad [14]. The spectra were acquired serially and the calibration was performed using the carbon-K peak at 284 eV.

3.2 CONVENTIONAL ANALYSIS.

3.2.1 Iron oxides. — Figure 2 shows the relevant region of the energy-loss spectrum of FeO with the edges O-K at 532 eV and Fe-L at 712 eV. We first perform the analysis in the standard way, with no deconvolution. The background is subtracted from each edge by performing a least-squares fit with a power law model on a part of the spectrum of width Γ immediately before the threshold. The choice of Γ is rather important in finding an accurate fit to the background and, following criteria of χ^2 minimization [14, 15], one finds that for such a spectrum, optimal values for Γ lie in the 70-90 eV range. Different parameters are generally found for the two edges handled separately. The next step is to integrate the signal S contained in the window Δ . The atomic concentration ratio is now given by

$$[Fe]/[O] = S_{Fe-L}/S_{O-K} \cdot k \quad (5)$$

where the 'k-factor' is $k = \sigma_{O-K}/\sigma_{Fe-L}$.

Two calculated sets of cross sections (Hartree Slater [3] or hydrogenic [4]) have been used. As the signals S_{Fe-L} and S_{O-K} can be measured over various values of Δ , the results $[Fe]/[O]$ can be displayed as function of Δ (Fig. 3), where the quoted errors are evaluated from statistical considerations [14]. In general, the values of the concentration ratio are fairly close to those expected from the chemical formulae, and when estimated over a typical energy window $\Delta = 100$ eV, it is almost possible to discriminate the different compositions without ambiguity (see Tab. I).

These general results however deserve further comments. These data have been obtained on specimens with typical thickness t of the order of λ_p (inelastic mean free path). The measured ratios are estimated from the simple law :

$$t/\lambda_p = \text{Log}(I_t/I_0) \quad (6)$$

where I_t = total spectrum intensity and I_0 = zero loss intensity. Multiple scattering effects are then non-negligible. Consequently, table I also contains the results of the analysis performed on deconvolved spectra, using either the Fourier ratio [16] or the Fourier log [17] algorithms [18]. These results are checked to converge within a few % of the expected values, and the phases Fe_2O_3 and Fe_3O_4 are then clearly distinguishable.

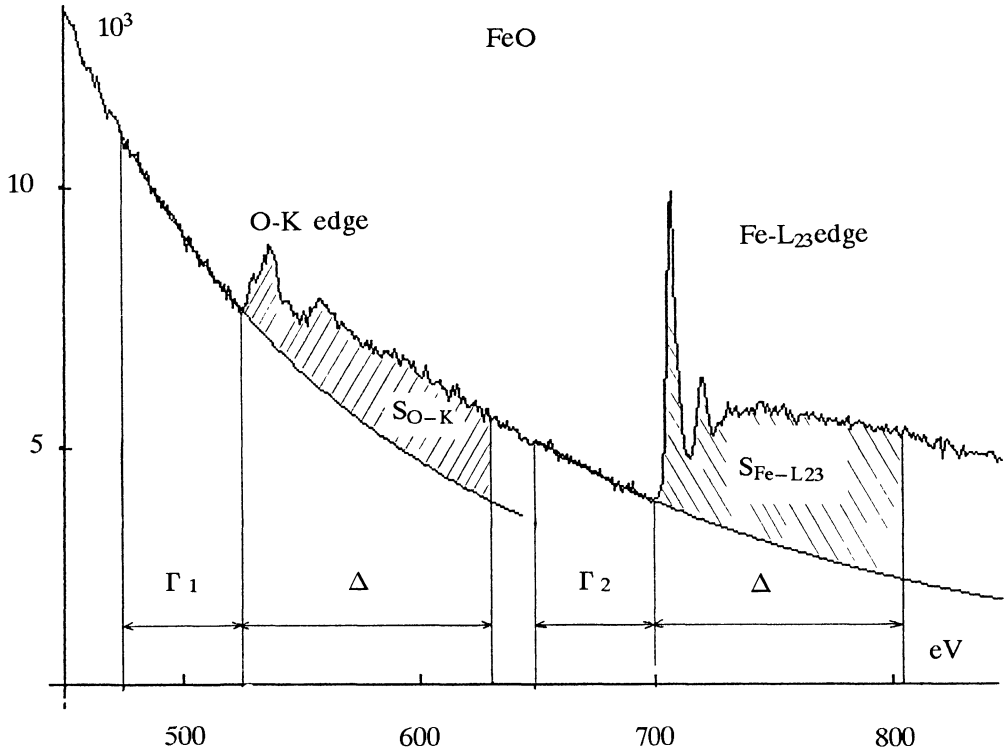


Fig. 2. — Determination of the oxygen and iron content in FeO by the conventional method, using the O-K and Fe-L edges. The background is subtracted from each edge and the resulting shaded areas are measured.

Another interesting aspect is the behaviour of the calculated ratios, $[\text{Fe}]/[\text{O}]$, as a function of Δ , see again figure 3. The Sigmak-Sigmals cross sections [4] provide more stable results. This is a consequence of the latest parametrization introduced by Egerton in the Sigmal2 software, to reproduce at least partially the shape of the differential L₂₃ cross section, with lines at threshold included. In contrast, the H.S. curves due to Rez, exhibit a slightly delayed profile which completely fails to model the white lines. The integrated cross section is thus too weak over the first 30 or 50 eV, and this gives rise to overestimated values for the concentration ratios. These H.S. data are not intended to be straightforwardly matched to the stripped signal, from threshold upwards.

To summarize, it appears that the conventional analysis, when used in conjunction with deconvolution methods and atomic cross sections due to Egerton, provides a rather satisfactory measure of the stoichiometry of this type of solid.

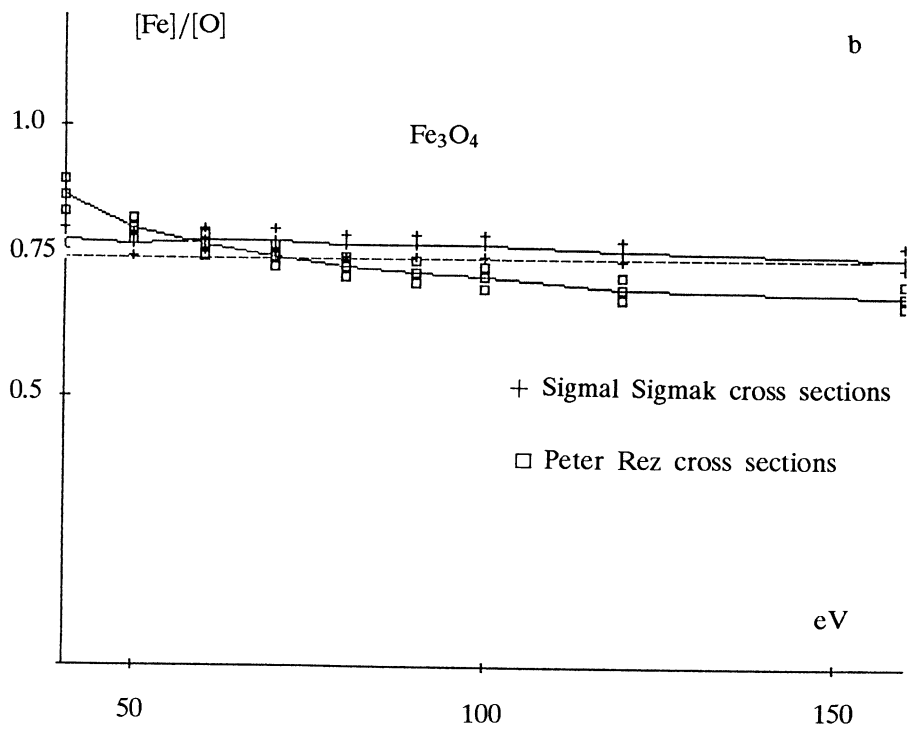
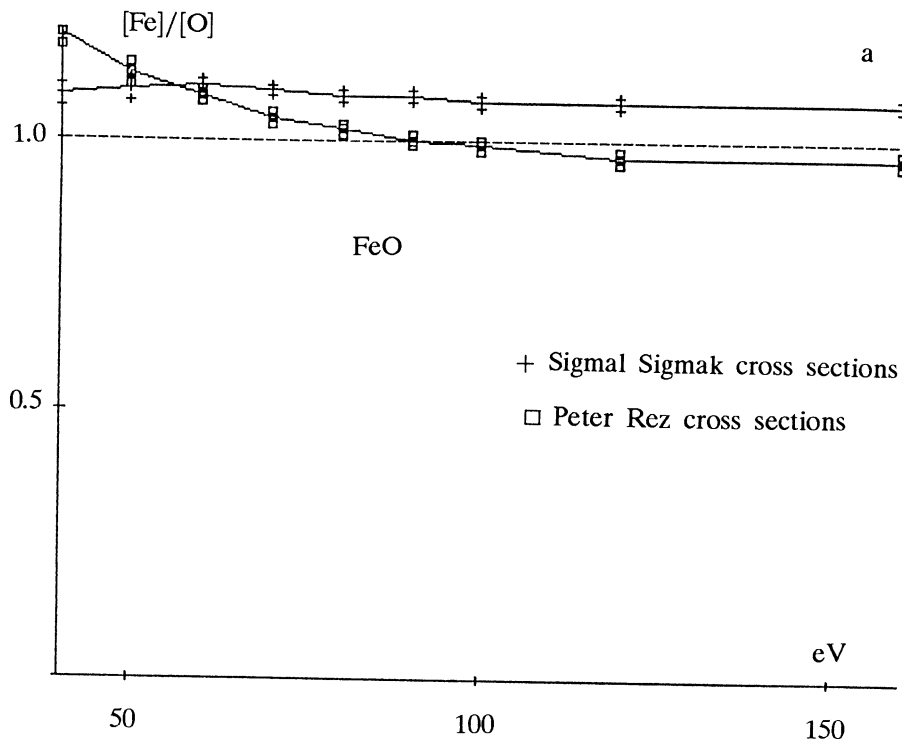


Fig. 3. — Values of $[Fe]/[O]$ as a function of Δ in iron oxides, determined using cross-sections calculated with the hydrogenic model (SIGMAK, SIGMAL) and the H-S method (P. Rez)

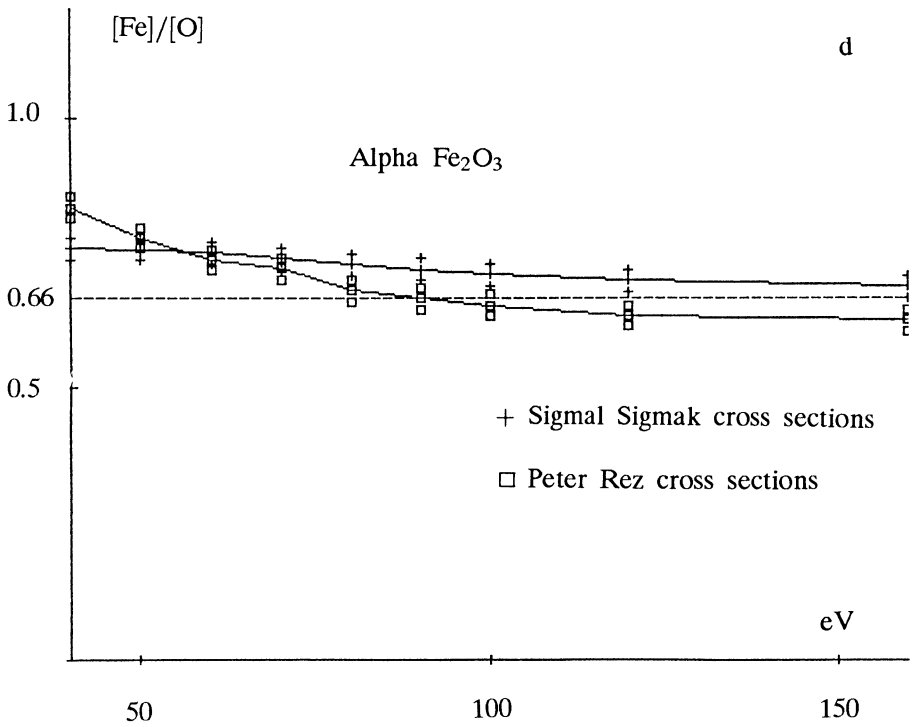
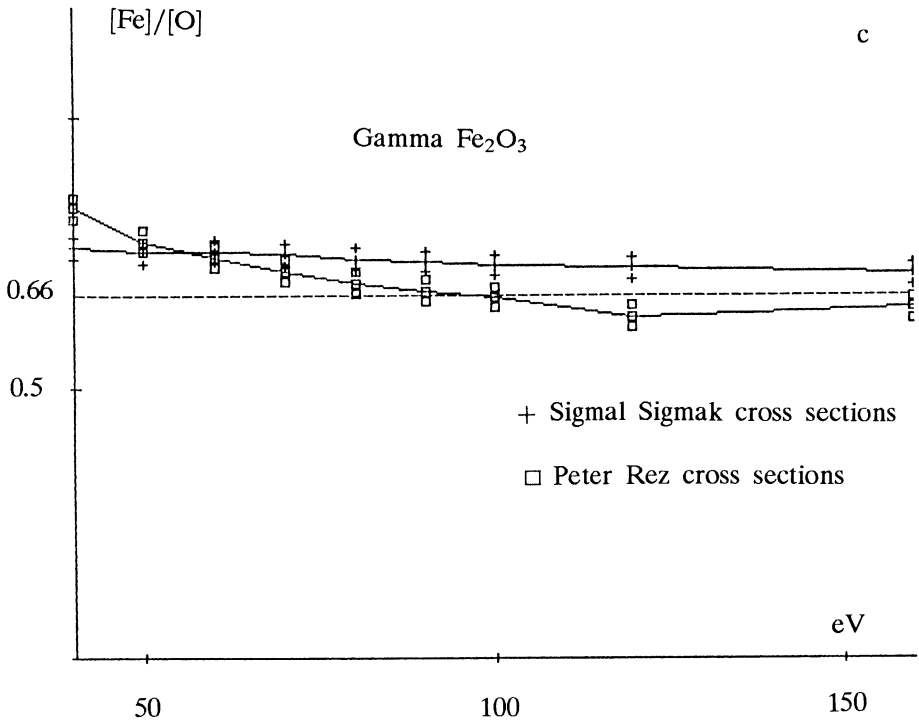


Fig. 3. — (continued).

Table I. — Values of $[\text{Fe}]/[\text{O}]$ in several iron oxides as measured by the background subtraction technique using raw experimental data, and data deconvolved using the Fourier-ratio and Fourier-log methods. Here $\Delta = 100$ eV.

Conventional method $\Delta = 100$ eV				
Spectrum analysed	FeO $t/\lambda = 1.0$	Fe ₃ O ₄ $t/\lambda = 1.09$	γ Fe ₂ O ₃ $t/\lambda = 1.12$	α Fe ₂ O ₃ $t/\lambda = 1.13$
Experimental	1,03 ± 0,06	0,76 ± 0,04	0,68 ± 0,04	0,71 ± 0,04
Fourier – Ratio deconvolved	1,00 ± 0,06	0,74 ± 0,04	0,67 ± 0,04	0,68 ± 0,04
Fourier – Log deconvolved	1,00 ± 0,07	0,75 ± 0,05	0,65 ± 0,04	0,68 ± 0,04

3.2.2 Chromium oxides. — Figure 4 shows the O-K and Cr-L edges of Cr₂O₃. The oxygen edge is seen to display considerable fine structure right up to the onset of the Cr signal. This means that a background subtraction using an AE^{-r} fit is difficult to perform, and is in any case not physically justified. We have nevertheless made several attempts to carry out the procedure using the small section of monotonically decreasing signal just before the Cr edge onset. E_2 was fixed as the last channel in which the signal was still decreasing (576 eV) and E_1 was varied between 571 eV (E'_1) and 573 eV (E_1). As can be seen in the figure, the resulting extrapolations differ widely as does the corresponding integration of the Cr signal. Also, the integration window for the O-K edge is restricted to 40 eV. The situation is similar in CrO₂.

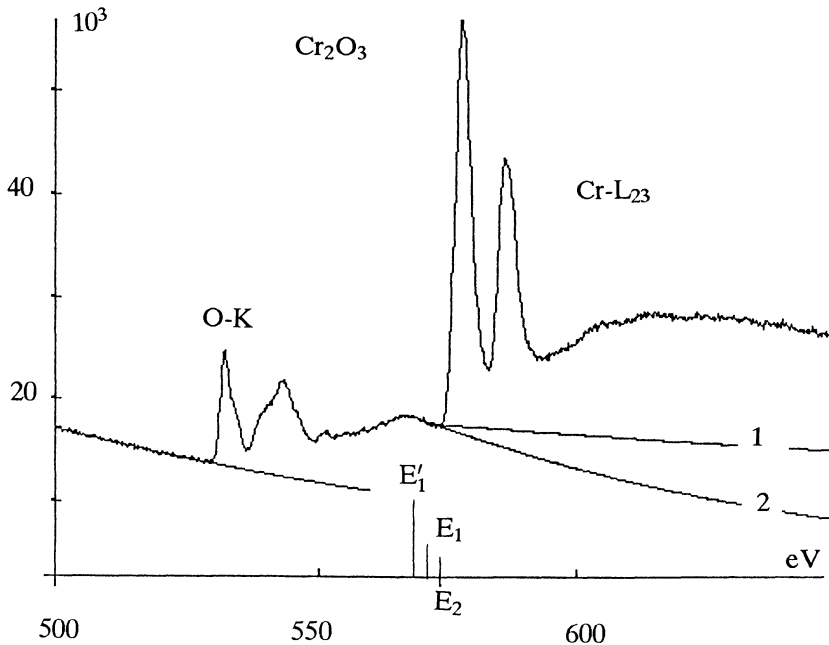


Fig. 4. — Subtraction of the background from the Cr-L edge in Cr₂O₃. The structure from the O-K edge means that there is little or no pre-edge region of the form AE^{-r} to extrapolate. The two very small windows used (E_1 to E_2 and E'_1 to E_2) give widely differing results, making accurate quantification impossible.

The resulting calculated stoichiometries vary rather widely, giving no clear idea of the composition of the solid. After deconvolution, the values are not more accurate and their overall scatter around the expected value is not reduced. Thus, using this method, a clear distinction cannot be made between the two phases, and a determination of the composition of an unknown phase would not be possible.

3.3 ANALYSIS USING THE NEW METHOD.

3.3.1 Iron oxides. — We will take as our general example in this case the same spectrum of FeO shown in figure 2. We first attempt to model the raw spectrum with no convolution or deconvolution, using the functions described in section 2. It has been found that the positions in energy of the Lorentz oscillators are very stable parameters in the fit. They quickly find their final values in the same place as the experimental peaks, even if initially chosen to be a few eV away from these. Therefore they are now usually fixed in this position throughout the calculation in order to speed up the process (the time required is proportional to the number of variable parameters). We also assume that the separation of the initial L_2 and L_3 levels is imposed as the separation between the L_2 and L_3 continuum contributions, and that the ratio of the weights of these two parts is fixed as $L_3/L_2 = 2$, the initial state occupancy ratio. All the other parameters mentioned in section 2 are left floating.

The result is shown in figure 5a. Clearly the agreement is not particularly close and the resulting value of $[Fe]/[O] = 1.6$ is very unsatisfactory. We therefore attempt three methods of including the effects of multiple scattering in the analysis. The first is the use of Fourier-ratio deconvolution of the experimental spectrum. This process requires the *a priori* removal of the background as in the conventional analysis, and so this part is left out of the resulting fit (Fig. 5c). The agreement is seen to be very much closer than in the previous case and the resulting value of $[Fe]/[O]$ is 1.07.

The second is the use of the Fourier-log deconvolution method. Here, the background remains, and the fit and deconvolved spectrum are shown in figure 5b. The agreement is possibly a little closer and the resulting value of $[Fe]/[O]$ is 0.98.

Finally we apply the method described earlier i.e. that of convolving the fit with the low-loss spectrum (Fig. 5d). To obtain the best fit from one set of initial conditions, the program requires 8 to 12 iterations and takes 10 to 20 minutes, all convolutions included, with the presently used LSI 11/73 host computer. To check the validity of the results, we have applied the method over a range of energy loss domains, covering 60 to 120 eV above the iron edge. At higher energies, the L_1 contribution must also be taken into account. The controlled features are the values of the (A, r) parameters and the position and weight of the H.S. cross sections. In the FeO case shown in figure 5d, the onset of the iron L_{23} H.S. contribution remains stable between 12.4 and 12.6 eV above the position of the first white line, and its relative weight with respect to the O-K term, does not vary by more than 1 or 2 %. The agreement with stoichiometry is again very close and we obtain $[Fe]/[O] = 0.99$. We have therefore applied this technique to the rest of the iron oxides. Table II shows the values found of the $[Fe]/[O]$ ratio for these oxides. The agreement with the expected values is in all cases very satisfactory, as it was when using the standard analysis.

Table II. — Values of $[Fe]/[O]$ as measured using the curve-fitting method with low-loss convolution.

Curve – fitting method			
	FeO	Fe ₃ O ₄	Fe ₂ O ₃
$[Fe]/[O]$	0.99 ± 0.03	0.73 ± 0.02	0.66 ± 0.02

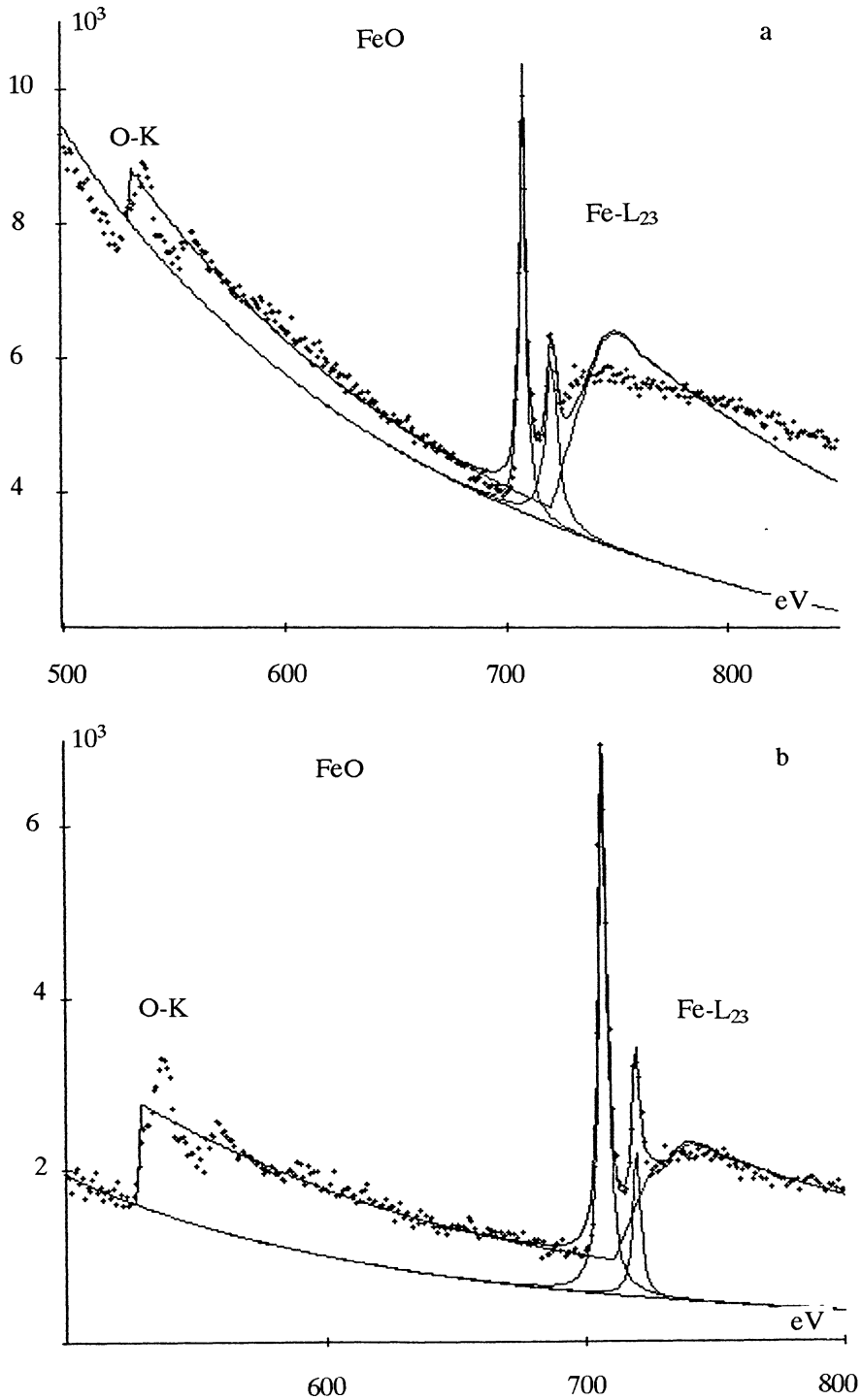


Fig. 5. — Attempts to model the O-K and Fe-L edges in FeO : (a) neglecting the effects of multiple scattering, (b) with the experimental data deconvolved with the low-loss spectrum using the Fourier-log method, (c) as (b) but using Fourier-ratio deconvolution, (d) convolving the calculated spectrum with the low-loss spectrum. The crosses are experimental points and the solid lines are the fit and its component parts.

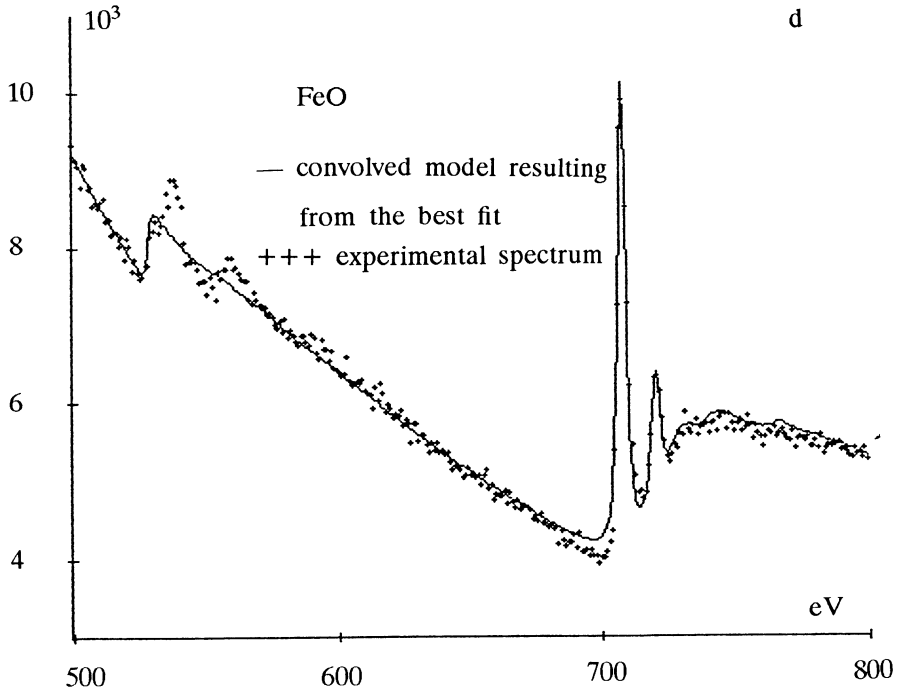
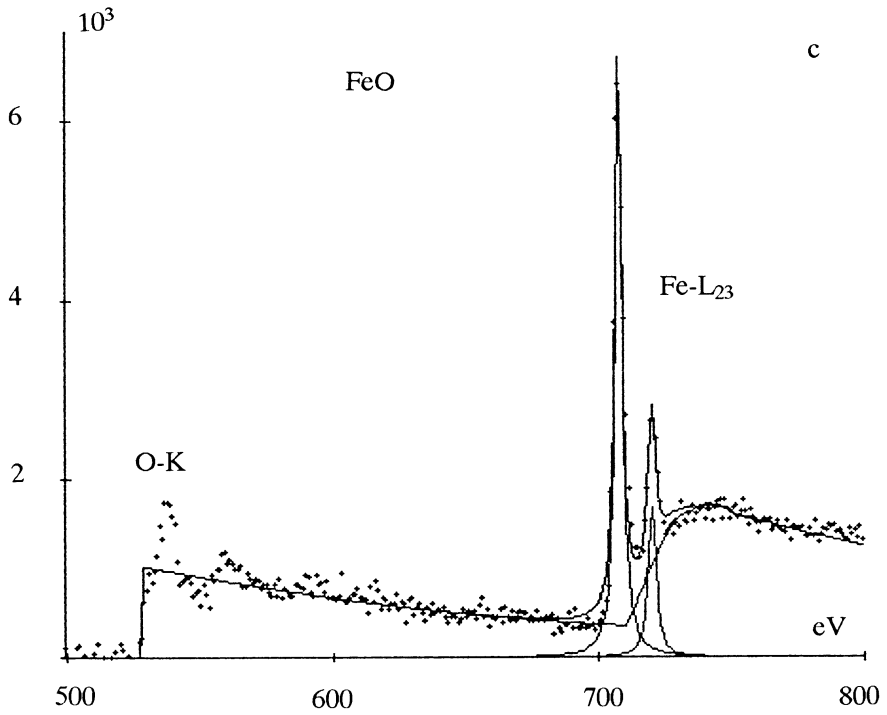


Fig. 5. — (continued).

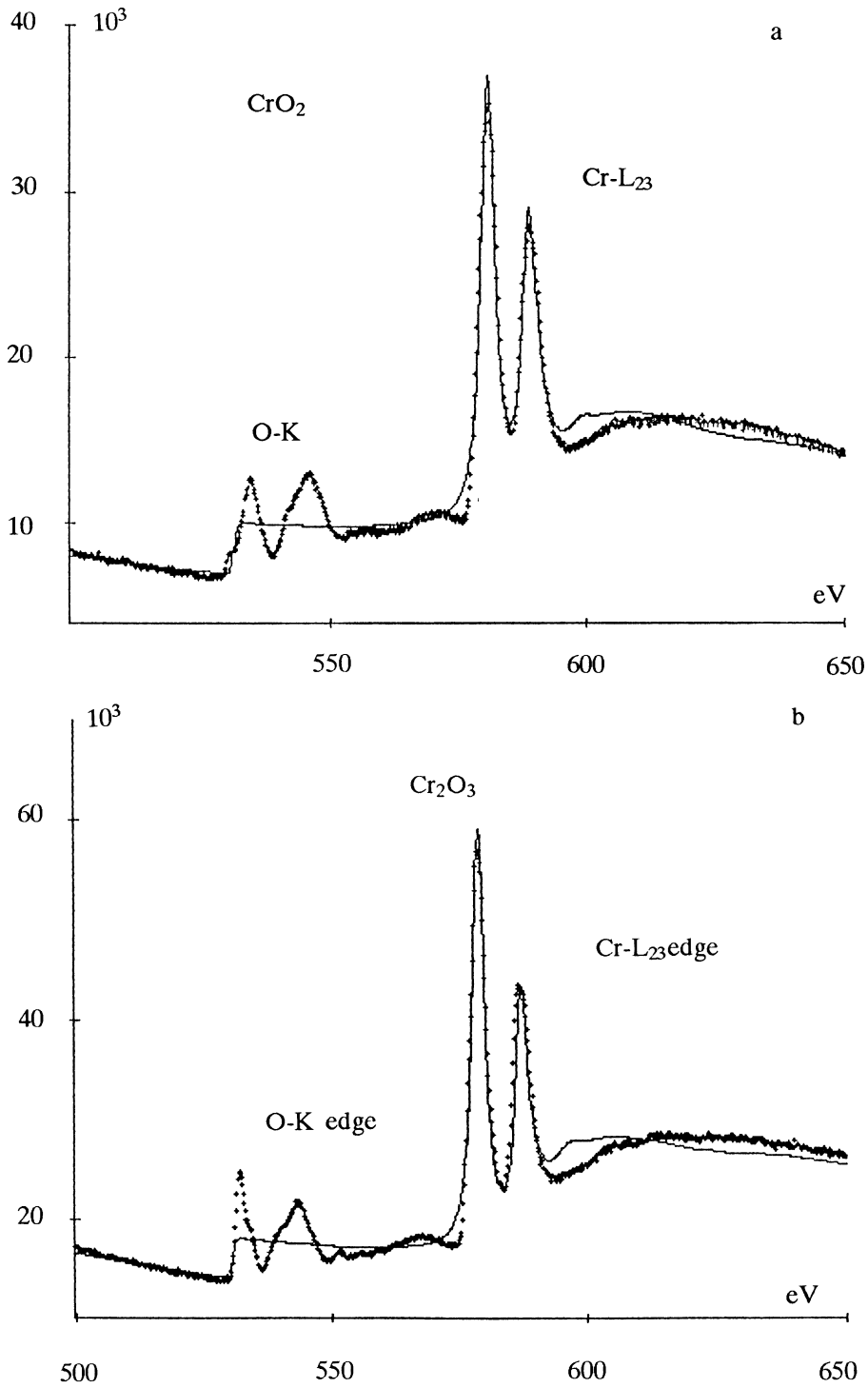


Fig. 6. — Modelling the O-K and Cr-L edges in chromium oxides by convolving the calculated spectrum with the low-loss region. The crosses are the experimental data and the solid lines are the convolved fits.

3.3.2 Chromium oxides. — The same procedure has been applied to the spectra of CrO_2 and Cr_2O_3 . The resulting convolved fits are shown in figure 6 and the atomic concentration ratios found are $[\text{Cr}]/[\text{O}] = 0.48 \pm 0.03$ and 0.64 ± 0.03 respectively. This is clearly a great improvement on the results obtained by the standard method, and a clear distinction is now possible between the two phases. It is worth noting that these values could be obtained when the initial weights used for each edge in the CrO_2 were chosen to correspond to those expected in Cr_2O_3 , and *vice-versa*, thus the process is not dependent on a prior knowledge of the stoichiometry.

3.4 DISCUSSION. — All three methods which take into account the multiple scattering effects yield satisfactory values for the atomic concentrations. The main advantage of the methods in which the experimental data are deconvolved is the speed of the calculations, the time being reduced by the fact that the deconvolution need only be performed once in each case, whereas the convolution of the fit must be performed after each iteration. However, the Fourier-ratio method has the disadvantage that the background must be subtracted from the edge region first, which is effectively the same as imposing the values of A and r at the beginning. This is a constraint which is not usually desirable since, as mentioned earlier, the form of the background can change over the range of the spectrum, and thus if it is to be modelled with a single function, that function should at least be the one which fits best over the entire range, and not just in the pre-edge region. In any case the Fourier-ratio method is known not to be very reliable in the case of thicker specimens, and can introduce ringing if great care is not taken in extrapolating the edge tail to zero at the high energy end of the data.

The Fourier-log method is in principle less sensitive to any thickness variations, but requires the spectrum to be acquired without a break in the range from zero up to well beyond the edges concerned. Also, the large dynamic range of EELS data usually means that a gain change is usually introduced at some energy, and this must be eliminated. The method is thus rather inconvenient for treating edges at medium or high energy-loss, but is probably preferable for those at less than about 250 or 300 eV.

On the other hand, the approach of convolving the fit with the low-loss spectrum does not require the data to be acquired over a particularly extended range, and has the further advantage that the experimental data remain untouched, and can therefore be confidently ascribed their appropriate weights in the fitting procedure on the basis of Poisson statistics, whereas after deconvolution these weights become somewhat approximate.

In the case of the iron oxides there is no great advantage in the new method, since the standard analysis, using Sigmak and Sigmal cross-sections, works very well as long as deconvolution is used. It would appear that the main interest in the new approach lies in the treatment of cases in which the edges are strongly overlapping. The quality of the agreement in the case of the chromium compounds is rather surprising in view of the fact that the small portion of the O-K edge which is visible in the spectrum displays considerable structure in both CrO_2 and Cr_2O_3 , none of which is reproduced at all in the calculated spectra. The reason for the success of the method is clearly the fact that the O-K edge also participates in the rest of the fit (up to more than 100 eV past its onset). This enables the oxygen signal to retain its importance in the analysis, even though in the raw data most of it is effectively hidden. Nevertheless, the method will obviously have to be applied to a wide variety of materials with strongly overlapping edges, before accuracy of the kind reported here can be confirmed as routinely available with the technique.

4. Conclusions.

We have demonstrated some new approaches in quantitative elemental analysis by EELS using curve-fitting methods, presenting as examples their application to some transition metal oxides. The accurate deconvolution of the experimental data, or convolution of the model with

the low-loss spectrum, has been shown to be crucial if accurate results are to be obtained from samples of the order λ_p in thickness. The curve fitting approach has been shown to produce markedly superior results to those obtainable by conventional analysis, when the edges involved are strongly overlapping.

Acknowledgements.

One of us (MGW) is grateful for a European Exchange Programme Fellowship. We acknowledge the collaboration of C. Ortiz (IBM San Jose) for supplying the iron oxide specimens, and the assistance of P. Rez (Arizona State University) and P. Trebbia (Université d'Orsay) at various stages in the development of the method.

References

- [1] COLLIEX C., *Adv. Opt. Electron Spectrosc.*, Eds. R. Barer and V. E. Cosslett (Academic Press) **9** (1984) 65.
- [2] EGERTON R. F., *Electron Energy-Loss Spectroscopy in the Electron Microscope* (Plenum), 1986.
- [3] LEAPMAN R. D., REZ P. and MAYERS D. F., *J. Chem. Phys.* **72** (1980) 1232 ;
REZ P., *Ultramicroscopy* **9** (1982) 283 ;
REZ P., *X-ray Spectrometry* **13** (1984) 55 ;
AHN C. C. and REZ P., *Ultramicroscopy* **17** (1985) 105 ;
REZ P., *Ultramicroscopy* **28** (1989) 16.
- [4] EGERTON R. F., *Ultramicroscopy* **4** (1979) 169 ;
EGERTON R. F., Proc. 39th Ann. EMSA Meeting, Ed. G. W. Bailey (Claitor's Publishing Baton Rouge, Louisiana) 1981 p. 198.
- [5] CROZIER P. A. and EGERTON R. F., AEM Workshop, EMAG '87, Ed. G. W. Lorimer (The Institute of Metals, London) 1988 p.103.
- [6] STEELE J. D., TITCHMARSH J. M., CHAPMAN J. N. and PATERSON J. H., *Ultramicroscopy* **17** (1985) 273.
- [7] SHUMAN H. and SOMLYO A. P., *Ultramicroscopy* **21** (1987) 23.
- [8] LEAPMAN R. D. and SWYT C. R., *Ultramicroscopy* **26** (1988) 393.
- [9] BEVINGTON P. R., *Data Reduction and Error Analysis for the Physical Sciences* (McGraw Hill, New York) 1969.
- [10] MANOUBI T., TENCÉ M. and COLLIEX C., *Ultramicroscopy* **28** (1989) 49.
- [11] MANOUBI T., REZ P. and COLLIEX C., *J. Elect. Spect. and Relat. Phenom.* **50** (1990) 1.
- [12] PEARSON D. H., FULTZ B. and AHN C. C., *Appl. Phys. Lett.* **53** (1988) 1405.
- [13] ORTIZ C., LIM G., CHEN M. M. and CASTILLO G., *J. Mat. Res.* **3** (1988) 344.
- [14] TREBBIA P., *Ultramicroscopy* **24** (1988) 399.
- [15] TREBBIA P. and MANOUBI T., *Ultramicroscopy* **28** (1989) 266.
- [16] JOHNSON D. W. and SPENCE J. C. H., *J. Phys.* **D7** (1974) 771.
- [17] SWYT C. R. and LEAPMAN R. D., *Microbeam Analysis*, Eds. A. D. Romig and J. I. Goldstein (San Francisco Press, San Francisco) 1985, p.45.
- [18] EGERTON R. F., WILLIAMS B. G. and SPARROW T. G., *Proc. Roy. Soc. Lond. A* **398** (1985) 395 ;
EGERTON R. F. and CROZIER P. A., *Scanning Microscopy Supplement 2 : Proc. 6th Pfeifferkorn Conference (Scanning Microscopy International, Chicago – AMF O'Hare 1988) 245.*